J. Fluid Mech. (2001), *vol.* 437, *pp.* 325–336. Printed in the United Kingdom

Interfacial periodic waves of permanent form with free-surface boundary conditions

By EMILIAN PĂRĂU[1,2] AND FREDERIC DIAS[3]

[1]Institut Non Linéaire de Nice, Nice, France

[2]Faculty of Mathematics, West University of Timişoara, Timişoara, Romania

[3]Centre de Mathématiques et de Leurs Applications,
Ecole Normale Supérieure de Cachan, France

(Received 15 September 2000 and in revised form 19 December 2000)

In a two-fluid system where the upper surface of the upper fluid is free, there are two independent modes of oscillation about the state of equilibrium, an 'internal' mode and an 'external' mode, which are described by two distinct dispersion curves. An efficient numerical scheme based on Fourier series expansions is used to calculate periodic waves of permanent form and of finite amplitude. Three kinds of waves are calculated: combination waves resulting from the interaction between an 'internal' mode and an 'external' mode with the same phase speed but wavelengths in a ratio of 2 (1:2 resonance), combination waves resulting from the interaction between a long 'internal' mode and a short 'external' mode with the same phase speed, and pure 'external' waves. It is shown that the 1:2 resonance, which is well-known for capillary–gravity surface waves and can profoundly affect wave field evolution, can affect pure gravity waves in a two-fluid system, but not in oceanic conditions. On the other hand, it is shown that the long/short wave resonance can occur in ocean-type conditions. Finally it is confirmed that pure external waves of finite amplitude behave like surface waves.

1. Introduction

The influence of internal waves on oceanic surface waves has been a subject of oceanographic interest for several decades. Likewise the possible importance of surface waves for the generation of internal waves has also been studied. To better understand such interactions, idealized internal-wave/surface-wave systems have been introduced theoretically and experimentally. The simplest model is a two-fluid system where the upper surface of the upper fluid is free. This system has two independent modes of oscillation about the state of equilibrium, an 'internal' mode and an 'external' (or 'surface') mode.†

Such a two-fluid system admits resonant interactions between external and internal modes, which play an important role in energy transfer processes. For example Ball (1964) considered resonant triads that couple two external modes and one internal mode, while Segur (1980) showed that triads coupling two internal modes and one external mode are also possible. In the experiments of Lewis, Lake & Ko (1974),

† In this paper the terminology external/internal is used to describe the independent modes of oscillation. The terminology free-surface/interfacial is used to describe waves along the free surface and the interface, respectively. For instance, if only the 'external' mode is excited, we talk about 'external' waves, both for the interfacial and the free-surface waves.

in which a mechanically generated surface wave packet interacts with a constant-amplitude interfacial wave, it was shown that matching the group velocity of the surface wave with the phase velocity of the interfacial wave leads to a resonance in the system. All these resonances are important from a dynamical point of view.

Two-fluid systems where the upper surface of the upper fluid is free also admit waves of permanent form. These waves can feel the influence of resonant interactions between external and internal modes. A clear illustration is given by Akylas & Grimshaw (1992), who studied internal waves in a density-stratified fluid. Their figure 2 provides a field observation of a wave resulting from the interaction between a long 'internal' mode and a short 'external' mode with the same phase speed. Walker (1973), who designed experiments to observe interfacial solitary waves, writes that the unavoidable presence of surface mode noise poses a serious problem. It is possible that the noise is only part of the problem and that in fact solitary waves interact with a short external mode.

In this paper we calculate periodic waves of permanent form that propagate in a two-fluid system with free-surface boundary conditions. In contrast to waves travelling along the interface between two homogeneous fluids in the rigid-lid approximation (Holyer 1979; Meiron & Saffman 1983; Grimshaw & Pullin 1986; Funakoshi & Oikawa 1986; Evans & Ford 1996), there has been relatively little numerical work on interfacial waves with free-surface boundary conditions, although they are truer to nature, at least in oceanic situations as pointed out by Evans & Ford (1996). The main reason is that interactions between external and internal modes make the calculations difficult. Moni & King (1995) have computed pure 'external' solitary waves. Michallet & Dias (1999) have computed combination solitary waves resulting from the interaction between a long internal mode and a short external mode.

In § 2 we formulate the inviscid two-layer problem. The dispersion relation and the conditions for resonant interaction between external and internal modes are studied in § 3. The numerical procedure is given in § 4. It is based on Fourier series expansions. Some results of the calculations are presented in § 5. Three cases are considered: combination waves resulting from the interaction between an internal mode and an external mode with the same phase speed but wavelengths in a ratio of 2 (1:2 resonance), combination waves resulting from the interaction between a long internal mode and a short external mode with the same phase speed, and pure external waves.

2. Formulation

Both fluids are inviscid. The flow is assumed to be irrotational in each layer. In the undisturbed state, both layers are at rest. The subscripts 1 and 2 refer to the lower and upper layers, respectively. The lower layer is of infinite depth while the upper layer is of thickness h. As we are interested in systems of travelling interfacial and free-surface waves of permanent form, it is convenient to adopt a reference frame moving with the speed c of the waves so that the flow is made steady and to use c to make velocities dimensionless. Since we only deal with periodic waves, the wavelength λ is used to make lengths dimensionless. The dimensionless coordinates are x (horizontal) and y (vertical). The following dimensionless numbers are introduced:

$$H = h/\lambda, \quad K = (2\pi/\lambda)h, \quad F = c^2/(gh), \quad F_\lambda = c^2/(g\lambda), \quad R = \rho_2/\rho_1,$$

where g is the acceleration due to gravity and ρ_i the fluid density in layer i.

In dimensionless form, the governing equations in each layer are

$$\Delta\phi_i = 0, \quad i = 1, 2, \tag{2.1}$$

where ϕ_i is the velocity potential in layer i. Along the interface described by $y = Y(x)$ there are two kinematic conditions

$$\frac{\partial\phi_i}{\partial x}\frac{\mathrm{d}Y}{\mathrm{d}x} - \frac{\partial\phi_i}{\partial y} = 0, \quad i = 1, 2. \tag{2.2}$$

Using Bernoulli's equation in each fluid and eliminating the pressure at the interface, one can write the dynamic condition in the form

$$\tfrac{1}{2}|\nabla\phi_1|^2 - \tfrac{1}{2}R|\nabla\phi_2|^2 + (1-R)\frac{1}{F_\lambda}Y = \tfrac{1}{2}(1-R) + \tfrac{1}{2}B_1. \tag{2.3}$$

Along the free surface described by $y = Y_s(x)$ there is the kinematic condition

$$\frac{\partial\phi_2}{\partial x}\frac{\mathrm{d}Y_s}{\mathrm{d}x} - \frac{\partial\phi_2}{\partial y} = 0. \tag{2.4}$$

Using Bernoulli's equation, one can write the free-surface dynamic condition in the form

$$\tfrac{1}{2}|\nabla\phi_2|^2 + \frac{1}{F_\lambda}Y_s = \tfrac{1}{2} + \frac{H}{F_\lambda} + \tfrac{1}{2}B_2. \tag{2.5}$$

The constants B_1 and B_2 are the unknown Bernoulli's constants. The mean level of the interface $y = Y(x)$ is chosen to be zero and we only consider symmetric waves. The waves are centred at $x = 0$ and therefore the study is restricted to values of x between 0 and $\frac{1}{2}$. The mean value condition on the interface is written as

$$\int_0^{1/2} Y(x)\mathrm{d}x = 0, \tag{2.6}$$

while the mean value of the free-surface elevation is written as

$$2\int_0^{1/2} Y_s(x)\mathrm{d}x = H. \tag{2.7}$$

The problem involves three independent parameters, which can be chosen as the Froude number F_λ based on the wavelength (or the Froude number F based on the upper layer thickness), the density ratio R and the ratio H between the thickness of the upper layer and the wavelength (or the wavenumber $K = 2\pi H$).

3. Conditions for resonant interaction between external and internal modes

Given waves of the form

$$\phi_1 = x + C\mathrm{e}^{2\pi y}\sin(2\pi x),$$
$$\phi_2 = x + [A\cosh(2\pi y) + B\sinh(2\pi y)]\sin(2\pi x),$$

where A, B and C are constants, the linearization of the problem (2.1)–(2.5) results in the wave profiles

$$Y = -C\cos(2\pi x), \tag{3.1}$$

$$Y_s = H - C\cos(2\pi x)\left[\cosh(2\pi H) + \sinh(2\pi H)\left(\frac{1}{R} - \frac{1-R}{2\pi R F_\lambda}\right)\right], \tag{3.2}$$

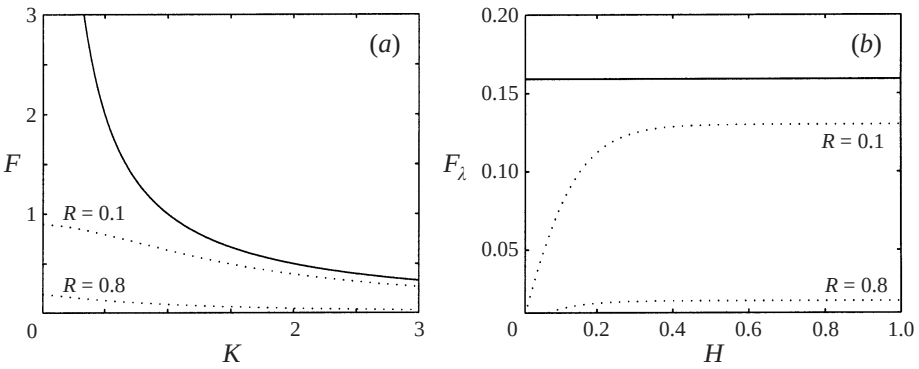

FIGURE 1. Dispersion curves for (3.3) in the (F, K)-plane (a) and in the (F_λ, H)-plane (b) for $R = 0.1$ and $R = 0.8$. The solid lines are the external modes. The dotted lines are the internal modes. The 'external' branch does not depend on R.

and in the dispersion relation (Lamb 1932, Article 231)

$$[1 + R\tanh(2\pi H)]F_\lambda^2 - \frac{F_\lambda}{2\pi}[1 + \tanh(2\pi H)] + \frac{1}{4\pi^2}(1 - R)\tanh(2\pi H) = 0. \quad (3.3)$$

Solving (3.3) for F_λ gives two solutions: the external mode F_λ^{e} and the internal mode F_λ^{i},

$$F_\lambda^{\mathrm{e}} = \frac{1}{2\pi}, \quad F_\lambda^{\mathrm{i}} = \frac{1}{2\pi}\frac{(1 - R)\tanh(2\pi H)}{1 + R\tanh(2\pi H)}, \quad (3.4)$$

or, rewritten in terms of the wavenumber $K = 2\pi H$ and the Froude number $F = F_\lambda/H$,

$$F^{\mathrm{e}} = \frac{1}{K}, \quad F^{\mathrm{i}} = \frac{1}{K}\frac{(1 - R)\tanh K}{1 + R\tanh K}. \quad (3.5)$$

Replacing F_λ by its value from (3.4) in (3.2) gives

$$Y_s^{\mathrm{e}} = H - C\cos(2\pi x)\mathrm{e}^{2\pi H} \quad \text{(external mode)}, \quad (3.6)$$

$$Y_s^{\mathrm{i}} = H + C\cos(2\pi x)\mathrm{e}^{-2\pi H}\left(\frac{1 - R}{R}\right) \quad \text{(internal mode)}. \quad (3.7)$$

One sees that the interface $y = Y(x)$ (3.1) and the free surface $y = Y_s^{\mathrm{e}}(x)$ (3.6) are in phase for the external mode while $y = Y(x)$ and $y = Y_s^{\mathrm{i}}(x)$ (3.7) are out of phase for the internal mode. Moreover external waves do not depend on the density ratio R: F_λ^{e} and Y_s^{e} are both independent of R.†

Both branches of the dispersion curve are plotted in figure 1, in the (K, F)-plane as well as in the (H, F_λ)-plane for $R = 0.1$ and $R = 0.8$. A density ratio of 0.1 is not encountered in nature but is used in this paper to illustrate some of the effects of the interactions between external and internal modes. Typical values of R in laboratory experiments are between 0.75 and 0.9. In oceanographic applications, the density ratio is close to unity (0.998 or so).

Looking at the dispersion curves in the (F, K)-plane, one sees that for a given internal mode of wavenumber K^{i} there is always a shorter external mode of wavenumber

† The fact that linear external waves do not depend on the density ratio is no longer true in the case of a lower layer of finite depth. On the other hand Lamb (1932) pointed out that this fact remains true in the case of an arbitrary number of liquids of different densities, arranged one over the other in horizontal strata, provided the uppermost surface be free, and the total depth infinite.

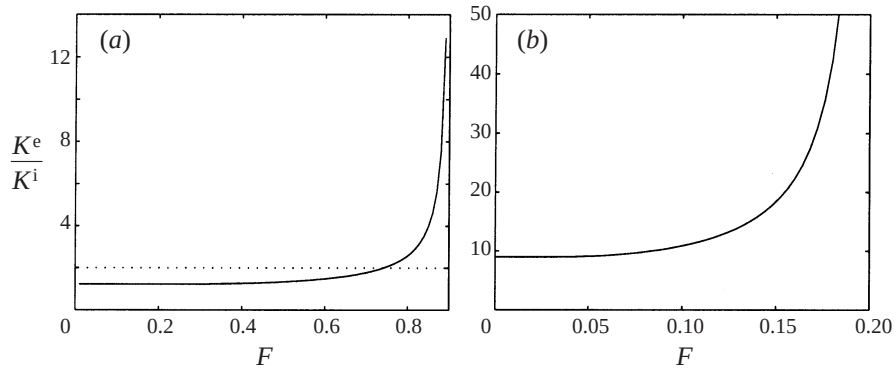

FIGURE 2. Ratio K^e/K^i of the wavenumbers of external and internal modes with the same phase speed vs. F for $R = 0.1$ (a) and $R = 0.8$ (b). The dotted line represents the 1:2 resonance.

K^e which moves with the same speed (same F). Whenever the ratio K^e/K^i is an integer the interactions between both modes become 'resonant', because they have the mathematical form of a resonantly forced, linear oscillator. The ratio K^e/K^i is plotted in figure 2 as a function of F for $R = 0.1$ and $R = 0.8$. When F approaches 0, the ratio tends towards $(1 + R)/(1 - R)$. When F approaches the Froude number of long internal waves ($\lim_{K\to 0} F^i$), the ratio K^e/K^i becomes infinite, because K^e is finite and $K^i = 0$.

Two special resonances are considered in this paper: the 1:2 resonance ($K^e = 2K^i$) and the 1:M resonance ($K^e = MK^i$) with M large. The 1:2 resonance is a special case of a resonant triad coupling one external mode and two (identical) internal modes. Our study is not directly applicable to oceanic applications since the 1:2 resonance in the two-layer model can only occur if $R < 1/3$. However, it may occur in a three-layer configuration with realistic density ratios. The dispersion relation for a three-layer system is given for example by Baines (1995). The behaviour of the ratio K^e/K^i as a function of F is qualitatively similar to those in figure 2 and one can show that

$$\lim_{F\to 0} \frac{K^e}{K^i} = \frac{1 - \rho_3/\rho_1 + \rho_2/\rho_1 - \rho_3/\rho_2}{1 - \rho_3/\rho_1 - \rho_2/\rho_1 + \rho_3/\rho_2},$$

where ρ_3 is the density of the top layer. Taking $\rho_2/\rho_1 = 0.99$ and $\rho_3/\rho_2 = 0.99$ (oceanic type conditions) or more generally $\rho_2/\rho_1 = \rho_3/\rho_2$ leads to a limit equal to 1. Therefore the 1:2 resonance can occur.

The 1:M resonance with M large corresponds to the resonance between a short external mode and a long internal mode. One of the consequences of this resonance is the appearance of short-wave oscillations at the tails of long internal waves. This resonance is realistic in oceanic conditions. Indeed a simple calculation in the limit $M \to \infty$ with $R = 0.99$ and $h = 100\,\mathrm{m}$ shows that long waves with ripples move at a speed of the order of $3\,\mathrm{m\,s^{-1}}$ and that the wavelength of the ripples is of the order of 6 m. A calculation with $R = 0.998$ gives $1.4\,\mathrm{m\,s^{-1}}$ for the speed and 1.3 m for the wavelength. In fact there is experimental evidence of such waves as mentioned in the introduction.

4. Numerical scheme for periodic waves

We follow the approach of Saffman & Yuen (1982) for computing interfacial waves in a rigid-lid configuration and extend it to a free-surface configuration. The method

is based on Fourier series expansions of the physical variables x and y in terms of the complex potential $\phi + \mathrm{i}\psi$. They give in the bottom layer

$$x_1 = \phi_1 + \sum_{n=1}^{N} a_n \sin(2\pi n\phi_1) \exp(2\pi n\psi_1), \tag{4.1}$$

$$y_1 = \psi_1 + a_0 + \sum_{n=1}^{N} a_n \cos(2\pi n\phi_1) \exp(2\pi n\psi_1), \tag{4.2}$$

and in the upper layer

$$x_2 = \phi_2 - \sum_{n=1}^{N} \sin(2\pi n\phi_2)[b_n \cosh(2\pi n\psi_2) - d_n \sinh(2\pi n\psi_2)], \tag{4.3}$$

$$y_2 = \psi_2 + b_0 - \sum_{n=1}^{N} \cos(2\pi n\phi_2)[b_n \sinh(2\pi n\psi_2) - d_n \cosh(2\pi n\psi_2)]. \tag{4.4}$$

The interface is described by $\psi_1 = \psi_2 = 0$. We write the potentials as

$$\phi_1 = \xi - s, \quad \phi_2 = \xi + s. \tag{4.5}$$

The unknown function s is expanded in a Fourier series

$$s(\xi) = \sum_{n=1}^{N-1} c_n \sin(2\pi n\xi). \tag{4.6}$$

Therefore along the interface one has

$$x_1 = \xi - s + \sum_{n=1}^{N} a_n \sin(2\pi n(\xi - s)), \quad Y_1 = a_0 + \sum_{n=1}^{N} a_n \cos(2\pi n(\xi - s)), \tag{4.7}$$

and

$$x_2 = \xi + s - \sum_{n=1}^{N} b_n \sin(2\pi n(\xi + s)), \quad Y_2 = b_0 + \sum_{n=1}^{N} d_n \cos(2\pi n(\xi + s)). \tag{4.8}$$

Along the free surface, described by $\psi_2 = \psi_s$, one has

$$x_2 = \phi_2 - \sum_{n=1}^{N} \sin(2\pi n\phi_2)[b_n \cosh(2\pi n\psi_s) - d_n \sinh(2\pi n\psi_s)], \tag{4.9}$$

$$Y_s = \psi_s + b_0 - \sum_{n=1}^{N} \cos(2\pi n\phi_2)[b_n \sinh(2\pi n\psi_s) - d_n \cosh(2\pi n\psi_s)]. \tag{4.10}$$

Of course, along the interface x_1 and Y_1 must be equal to x_2 and Y_2, respectively. We discretize ξ as

$$\xi_i = \frac{i-1}{2N}, \quad i = 1, \ldots, N+1. \tag{4.11}$$

The resulting system of equations consists of $(N-1)$ equations $x_1 = x_2$ (at the end points, it is automatically satisfied), $(N+1)$ equations $Y_1 = Y_2$, $(N+1)$ Bernoulli's equations along the interface, $(N+1)$ Bernoulli's equations along the free surface and the zero mean value condition (2.6). The $(4N+3)$ unknowns are the Bernoulli's

constants B_1 and B_2, the coefficients a_n ($n = 0, \ldots, N$), the coefficients b_n ($n = 0, \ldots, N$), the coefficients d_n ($n = 1, \ldots, N$) and the coefficients c_n ($n = 1, \ldots, N-1$).

Written explicitly, the mean value condition becomes

$$\int_0^{1/2} Y_1 \frac{\mathrm{d}x_1}{\mathrm{d}\xi}\mathrm{d}\xi = 0 \quad \text{or} \quad \int_0^{1/2} Y_2 \frac{\mathrm{d}x_2}{\mathrm{d}\xi}\mathrm{d}\xi = 0. \tag{4.12}$$

The relative thickness of the upper layer is $H = \psi_s + b_0$. The system is solved by Newton's method. In Michallet & Dias (1999) the size of the system was of the order $5N$ while it is only of order $4N$ with the present method. However, like other methods based on Fourier series expansions it is not adequate to compute large-amplitude waves.

5. Some numerical results

The numerical scheme described in §4 is used to compute solutions for several values of the three independent parameters of the problem: the Froude number F, the density ratio R and the dimensionless wavenumber K. We focus our attention on two values of R, 0.1 and 0.9, and we study three cases: (i) the 1:2 wave resonance (only when $R = 0.1$), (ii) combination waves resulting from the interaction between a short external mode and a long internal mode – for these waves, which approximate solitary waves with ripples, K is small and F is slightly above $F^{\mathrm{i}}(K)$ defined in (3.5) – and (iii) 'external' periodic waves – for these waves, K is unrestricted and F is larger than $F^{\mathrm{e}}(K)$ defined in (3.5).

5.1. *The second-harmonic resonance*

As mentioned above, the second-harmonic resonance between an external mode and an internal mode can occur when $R < 1/3$. But it can also occur in realistic conditions if a third layer is added (the code can be easily extended to a three-layer configuration). When $R = 0.1$ the resonance takes place at $K^{\mathrm{i}}_{1:2} = 0.675$, $F^{\mathrm{i}}_{1:2} = 0.741$. We compute solutions in the neighbourhood of this point. The number of mesh points is of the order of 20 because it is difficult to increase the number of points. The reason is that terms like $\cosh(2\pi n\psi_s)$ and $\sinh(2\pi n\psi_s)$ in (4.9) and (4.10), which behave like $\cosh(nK)$ and $\sinh(nK)$ for large n, explode rapidly as n increases. But $N = 20$ is enough to describe waves of moderate amplitude. In the case of capillary–gravity surface waves, Schwartz & Vanden-Broeck (1979) found that $N = 30$ was adequate for 'easy' profiles.

Results are shown in figure 3 for $K < K^{\mathrm{i}}_{1:2}$ ($K = 0.64$) and in figure 4 for $K > K^{\mathrm{i}}_{1:2}$ ($K = 0.706$). As the wave amplitude increases, the wave goes from a pure linear 'internal' wave to a combination wave mixing the internal and the external modes. When $K < K_{1:2}$ the speed decreases with amplitude. When $K > K_{1:2}$ it is the opposite.

Combination waves can bifurcate into a pure external wave as shown in figures 5 and 6. The parameters for the various plots of figures 3–6 are summarized in figure 7. The curve along which a combination wave bifurcates into a pure external wave is indicated as well. This curve is in fact very close to the curve $F = 1/(2K)$, which is the external branch of the dispersion curve (3.3) evaluated at a wavenumber $2K$ instead of K.

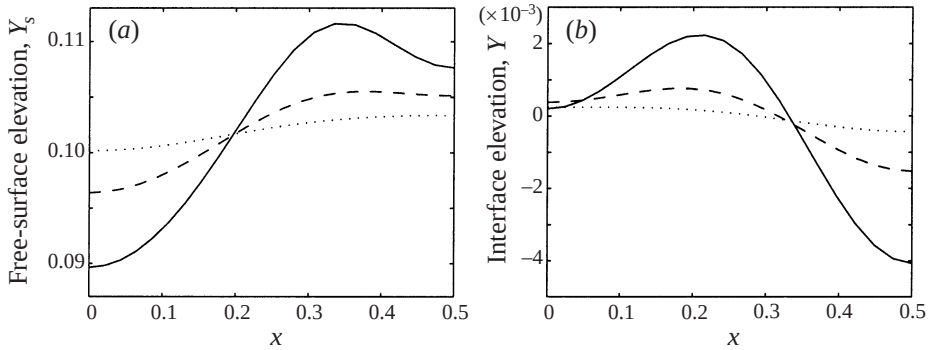

FIGURE 3. Profiles of the free surface (a) and of the interface (b) in a neighbourhood of the second-harmonic resonance. The parameters are $R = 0.1$ and $K = 0.64$. Three profiles with $F = 0.733$ (—), $F = 0.743$ (– –) and $F = 0.75$ ($\cdots$) are shown. When $F = 0.75$ the waves are almost pure linear internal waves and consequently the interface and the free surface are out of phase, in agreement with the results of § 3.

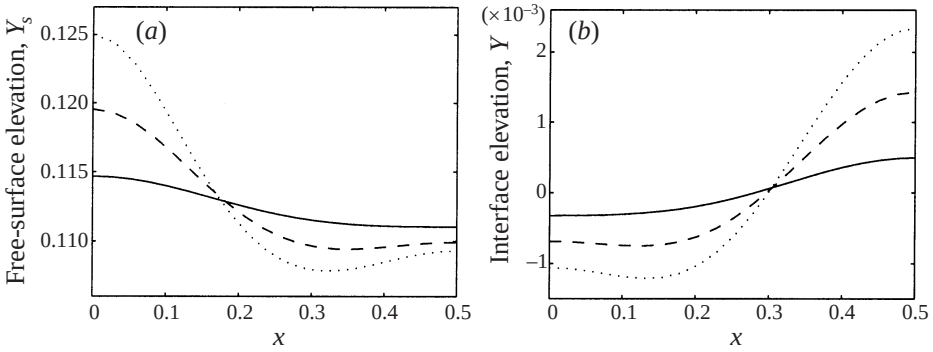

FIGURE 4. Same as figure 3 but with $K = 0.706$; $F = 0.734$ (—), 0.747 (– –) and 0.765 ($\cdots$). When $F = 0.734$ the waves are almost pure linear internal waves and therefore are out of phase.

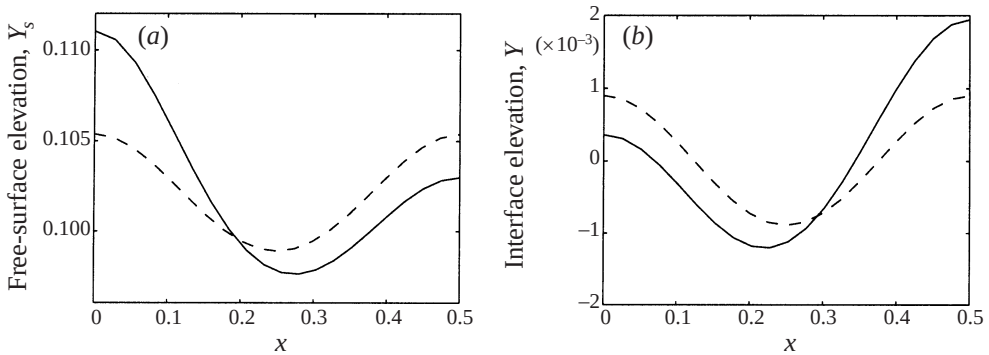

FIGURE 5. Profiles of the free surface (a) and of the interface (b) near and at the bifurcation from a combination wave into a pure external wave: $K = 0.64$ with $F = 0.794$ (—) and $F = 0.781$ (– –). The pure external waves (– –) are in phase.

5.2. *Long waves with ripples resulting from the interaction between a long internal mode and a short external mode*

The computations in this case were generally performed with $N = 160$ or 200 mesh points. We checked that the results are independent of the number of mesh points

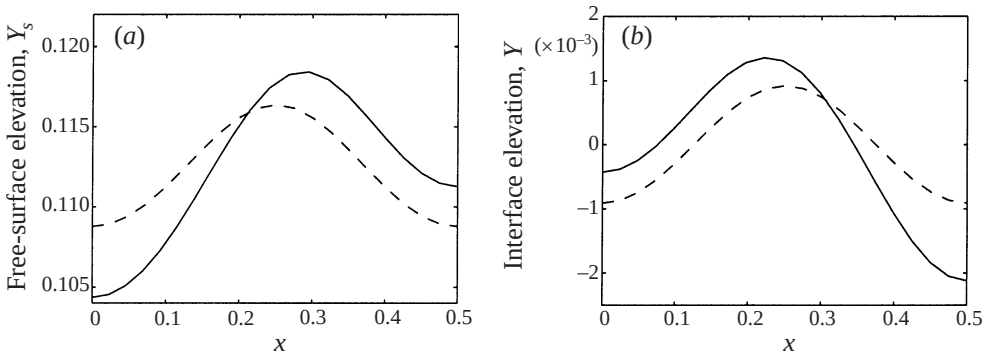

FIGURE 6. Same as figure 5 but with $K = 0.706$; $F = 0.702$ (—) and $F = 0.709$ (– –).

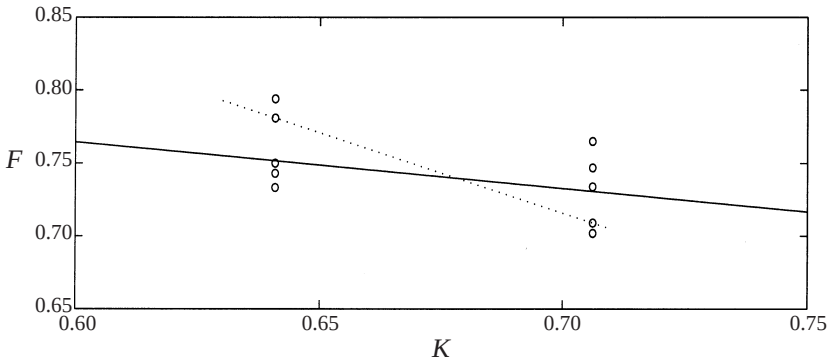

FIGURE 7. The 1:2 resonance in the (K, F)-plane. The circles (○) represent the solutions plotted in figures 3–6. The solid line is the internal branch of the dispersion curve (3.3). The dotted line is the curve along which a combination wave bifurcates into a pure external wave.

within graphical accuracy. Long waves have already been computed by Michallet & Dias (1999). However the numerical scheme is different and in the present computations the bottom layer is unbounded. Moreover we can now follow the branches of long waves with ripples all the way up to their bifurcation into a short wave. For long waves, H is small (typically $H \in [0.005, 0.01]$).

Typical profiles are shown in figure 8. The free-surface solitary pulse is always of elevation while the interfacial pulse is of depression. The free-surface ripples are in phase with the interfacial ripples.

If K^e denotes the wavenumber of the ripples obtained from the dispersion relation (3.3) for a given F_λ, we observe that for $M < K^e/K < M + 1$ (M integer) we have a family of solutions characterized by the the same number of ripples. For $K^e/K \approx M + 1/2$ the minimum amplitude of the ripples for such a family of solutions is reached (see figure 8). When $K^e/K \approx M$ the solutions are more difficult to obtain. They could not be obtained by Michallet & Dias (1999). In this case the ripple amplitude increases to the amplitude of the solitary pulse and the long wave with ripples becomes an external wave of wavenumber close to K^e. It is not exactly K^e because there is a nonlinear correction to the wavenumber due to the finite amplitude of the ripples. The bifurcation of a long wave with ripples into a short external wave is shown in figure 9. One sees that there are two short waves with M oscillations which can appear when $K^e/K \approx M$. As an example take $M = 24$.

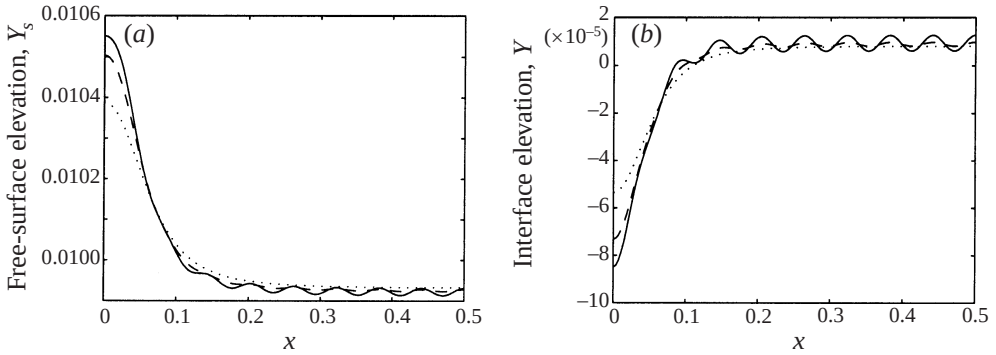

FIGURE 8. Profiles of the free surface and of the interface for $R = 0.1$, $H = 0.01$ and three values of the Froude number: $F_\lambda = 0.0092$ (dotted), 0.0093 (dashed), 0.00935 (solid). The corresponding ratios of the wavenumbers K^e/K are 17.3, 17.11 and 17.02, respectively. The corresponding values of F are 0.92, 0.93 and 0.935.

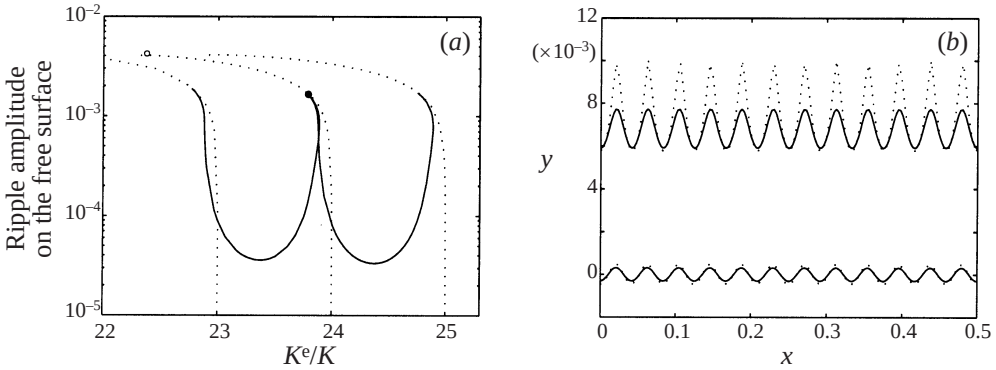

FIGURE 9. The parameters are $R = 0.1$, $F = 1$. (*a*) As the ripple amplitude increases along the branch of long waves with ripples (—), the long waves bifurcate into a short external wave indicated by the dot. Only the amplitude of the free-surface ripples is shown because the same behaviour occurs along the interface. The branches of short waves (· · ·) are indicated all the way up to the limiting configuration. (*b*) Profiles (—) of the short free-surface and interfacial waves obtained as the limit of long waves with ripples along the branch $K^e/K \approx 24$ (see the dot in (*a*)). The value of H is 0.0067. A system of short waves close to the limiting configuration is shown as well (· · ·) (see the circle in (*a*)).

If one approaches $K^e/K \approx 24$ from the right, the limit is a periodic wave with 24 oscillations, with a trough at the ends and consequently at the origin as shown in figure 9. If one approaches $K^e/K \approx 24$ from the left, the limit is a periodic wave with 24 oscillations, with a crest at the ends and consequently at the origin. The branch of short external waves is shown as well in figure 9.

Since the short waves remain in phase along the free surface and the interface, the curvature at the origin must change sign along either the free surface or the interface as one moves along the branch of long waves with ripples (see the formation of a dip along the free surface in figure 10*a*). Another comment is that the amplitude of the free-surface solitary pulse is greater than the amplitude of the interfacial pulse for $R = 0.1$, and this is also true for the amplitudes of the ripples. For $R = 0.9$ the situation is the opposite (see figure 10*b*). For $R = 0.9$ we were not able to compute long waves with ripples of arbitrary amplitude, because the ratio K^e/K is quite large.

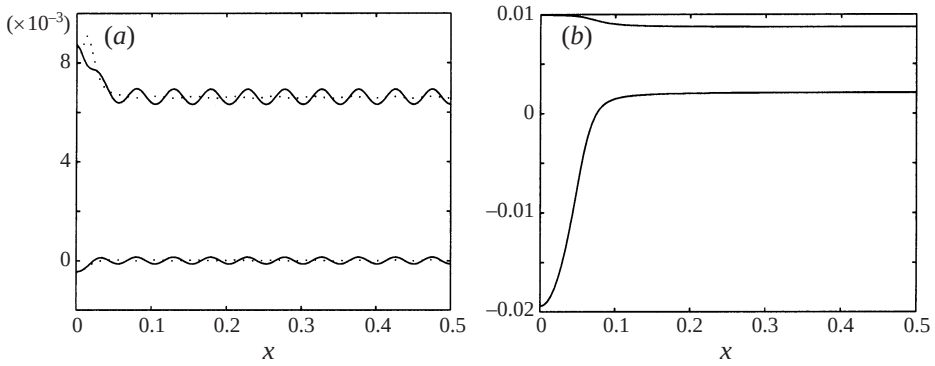

FIGURE 10. Profiles of long free-surface and interfacial internal waves for two density ratios. (*a*) $R = 0.1$, $H = 0.0067$; $F_\lambda = 0.0078$ (—) and 0.0083 ($\cdots$); (*b*) $R = 0.9$, $H = 0.0075$, $F_\lambda = 0.002$ ($K^e/K \approx 79.57$).

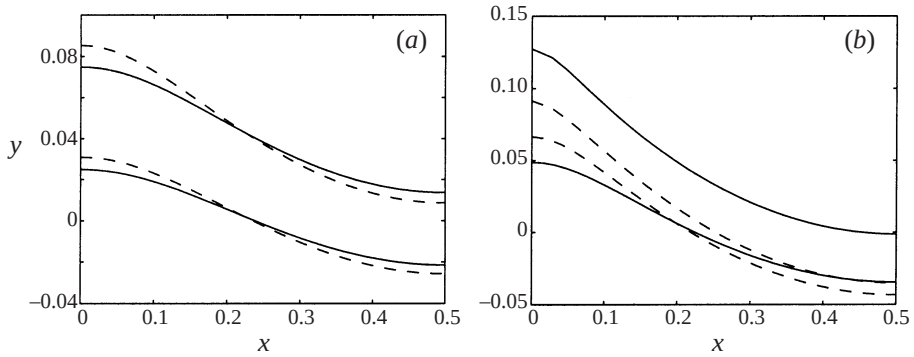

FIGURE 11. Profiles of interfacial and free-surface 'external' periodic waves. (*a*) $H = 0.04$, $F_\lambda = 0.165$; $R = 0.9$ (—) and 0.1 (——). (*b*) $R = 0.9$, $H = 0.04$, $F_\lambda = 0.186$ (—) and $R = 0.1$, $H = 0.01$, $F_\lambda = 0.18$ (——).

The situation is even worse if we take $R = 0.998$. Indeed the total number of mesh points becomes prohibitive if one wants to have enough mesh points in each ripple.

5.3. *External periodic waves*

Equation (3.3) shows that the dispersion relation of external waves is the same as the dispersion relation of deep-water surface waves. Therefore it is not surprising that external waves behave like deep-water surface waves. For example the speed of external periodic waves increases with amplitude. Consequently external waves lie above the curve $F = F_\lambda^e$ in figure 1. For the reason discussed in § 5.1 we only studied in detail long waves ($H \leqslant 0.04$) with a number of mesh points between 60 and 100. For larger values of H, solutions can be obtained with a smaller number of mesh points (for example, for $H = 0.1124$, the scheme works with $N = 20$).

Figure 11 shows various waves obtained with $R = 0.1$ or 0.9 and F_λ larger than F_λ^e. Overall, external waves behave like surface waves. The interface and the free surface are always in phase. Figure 11(*a*) shows that nonlinear external waves depend slightly on the density ratio R, as opposed to linear external waves which are independent on R. A final remark is that the code can be used to compute external periodic waves even if $R > 1$ since F^e is independent of R. But such waves are most likely unstable.

6. Conclusion

The rigid-lid approximation is commonly used to compute interfacial waves in a two-fluid system. However this approximation is too restrictive in certain circumstances and the rigid lid must be replaced by a free surface. In this paper interfacial periodic waves of permanent form with free-surface boundary conditions have been calculated. For density ratios less than 1/3, combination waves resulting from the interaction between an 'internal' mode and an 'external' mode with the same phase speed but wavelengths in a ratio of 2 (1:2 resonance) can exist. Density ratios less than 1/3 are not commonly found in nature or in laboratory experiments but we have shown that the 1:2 resonance can occur in a three-layer system with density ratios typical of those found in nature or in laboratory experiments. For all density ratios, combination waves resulting from the interaction between a long 'internal' mode and a short 'external' mode with the same phase speed can exist. These long waves are characterized by short-wave oscillations in their tails. We expect them to be found in oceanic conditions. Numerical difficulties were encountered when computing waves in ocean-type conditions, due to the large difference in length scales between the long internal mode and the short external mode. Finally it was shown that pure external waves behave like surface waves.

The authors thank the referees for suggestions which have hopefully made the paper more readable.

REFERENCES

Akylas, T. R. & Grimshaw, R. H. J. 1992 Solitary internal waves with oscillatory tails. *J. Fluid Mech.* **242**, 279–298.

Baines, P. G. 1995 *Topographic Effects in Stratified Flows.* Cambridge University Press.

Ball, F. K. 1964 Energy transfer between external and internal gravity waves. *J. Fluid Mech.* **19**, 465–478.

Evans, W. A. B. & Ford, M. J. 1996 An integral equation approach to internal (2-layer) solitary waves. *Phys. Fluids* **8**, 2032–2047.

Funakoshi, M. & Oikawa, M. 1986 Long internal waves of large amplitude in a two-layer fluid. *J. Phys. Soc. Japan* **55**, 128–144.

Grimshaw, R. H. J. & Pullin, D. I. 1986 Extreme interfacial waves. *Phys. Fluids* **29**, 2802–2807.

Holyer, J. Y. 1979 Large amplitude progressive interfacial waves. *J. Fluid Mech.* **93**, 433–448.

Lamb, H. 1932 *Hydrodynamics*, 6th edn. Cambridge University Press.

Lewis, J. E., Lake, B. M. & Ko, D. R. S. 1974 On the interaction of internal waves and surface gravity waves. *J. Fluid Mech.* **63**, 773–800.

Meiron, D. I. & Saffman, P. G. 1983 Overhanging interfacial gravity waves of large amplitude. *J. Fluid Mech.* **129**, 213–218.

Michallet, H. & Dias, F. 1999 Numerical study of generalized interfacial solitary waves. *Phys. Fluids* **11**, 1502–1511.

Moni, J. N. & King, A. C. 1995 Interfacial solitary waves. *Q. J. Mech. Appl. Maths* **48**, 21–38.

Saffman, P. G. & Yuen, H. C. 1982 Finite-amplitude interfacial waves in the presence of a current. *J. Fluid Mech.* **123**, 459–476.

Schwartz, L. W., Vanden-Broeck, J.-M. 1979 Numerical solution of the exact equations for capillary-gravity waves. *J. Fluid Mech.* **95**, 119–139.

Segur, H. 1980 Resonant interactions of surface and internal gravity waves. *Phys. Fluids* **23**, 2556–2557.

Walker, L. R. 1973 Interfacial solitary waves in a two-fluid medium. *Phys. Fluids* **16**, 1796–1804.